Title
Effect of Growth Induced (Non)Stoichiometry on the Structure, Dielectric Response, and Thermal Conductivity of SrTiO3 Thin Films

Journal
Chemistry of Materials, 24(2)

ISSN
0897-4756

Authors
Breckenfeld, E
Wilson, R
Karthik, J
et al.

Publication Date
2012-01-24

DOI
10.1021/cm203042q

Peer reviewed

CHEMISTRY OF MATERIALS

Article

pubs.acs.org/cm

Effect of Growth Induced (Non)Stoichiometry on the Structure, Dielectric Response, and Thermal Conductivity of $SrTiO_3$ Thin Films

E. Breckenfeld, R. Wilson, J. Karthik, A. R. Damodaran, D. G. Cahill, and L. W. Martin*

Department of Materials Science and Engineering and Materials Research Laboratory, University of Illinois, Urbana−Champaign, Urbana, Illinois 61801, United States

Supporting Information

ABSTRACT: We report dramatic variations in cation stoichiometry in $SrTiO_3$ thin films grown via pulsed laser deposition and the implications of this nonstoichiometry for structural, dielectric, and thermal properties. The chemical composition of $SrTiO_3$ thin films was characterized via X-ray photoelectron spectroscopy and Rutherford backscattering spectrometry. These studies reveal that deviations in laser fluence and deposition geometry can result in deviations of cation stoichiometry as large as a few percent. Additionally, X-ray diffraction was used to probe structural evolution and revealed an asymmetric strain relaxation mechanism in which films possessing Sr-excess undergo relaxation before those possessing Sr-deficiency. Furthermore, the dielectric constant decreases and the loss tangent increases with increasing nonstoichiometry with intriguing differences between Sr-excess and -deficiency. Thermal conductivity is also found to be sensitive to nonstoichiometry, with Sr-excess and -deficiency resulting in 65% and 35% reduction in thermal conductivity, respectively. These trends are explained by the expected defect structures.

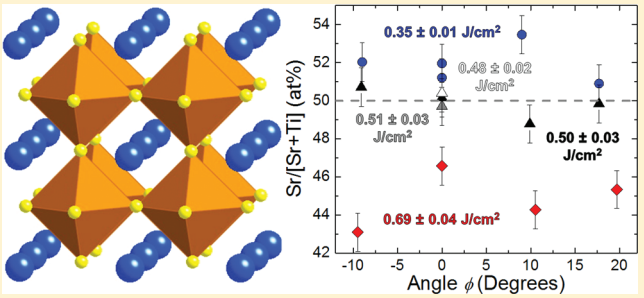

KEYWORDS: *pulsed laser deposition, $SrTiO_3$, dielectric, thermal conductivity, thin films*

INTRODUCTION

For decades, oxide materials such as $SrTiO_3$ have been considered for electronic, dielectric, and thermoelectric applications. The static dielectric permittivity (ε_r) of $SrTiO_3$ is ∼300 at room temperature and rapidly increases upon cooling to the quantum paraelectric state.[1] Likewise, $SrTiO_3$ has drawn attention as a candidate material for thermoelectrics based on its large carrier effective mass and resulting large thermopower.[2−4] More generally, $SrTiO_3$ is one of the most widely studied perovskite oxides and is highly susceptible to donor-doping by cationic substitution, oxygen vacancies, and field effects that result in a dramatic range of transport properties.[5−8]

More recently, researchers have been doggedly pursuing one of the most exciting discoveries in the study of $SrTiO_3$—the development of unexpected phenomena at the heterointerface between $LaAlO_3$ and $SrTiO_3$. Since the seminal discovery of a conducting state at such heterointerfaces in 2004,[9] researchers have made a number of exciting findings related to these interfaces including the observation of magnetic ground states,[10] superconductivity,[11] and built-in polarizations.[12] Researchers have incorporated these interfaces on silicon wafers[13] by synthesizing high-quality $LaAlO_3$ and $SrTiO_3$ thin films and have demonstrated electric-field writing of insulating and conducting states at the nanometer-scale.[14] Among the more pressing challenges facing researchers in this field is answering the question of whether these exotic phenomena are the result of intrinsic electronic effects or if they arise because of spurious effects in the samples. It has been hypothesized that the alternating planes of LaO^+ and AlO^{2-} in $LaAlO_3$ build up an electrostatic potential thereby driving electrons to occupy Ti 3d states in the nearby $SrTiO_3$ that, in turn, forms 2-dimensional bands parallel to the interface.[15] Alternative models have been proposed including conductivity derived from oxygen vacancies[10,16] or from intermixing of cations across these interfaces and the formation of n-type conducting La-doped $SrTiO_3$.[17] Recent studies have investigated the extent of cation intermixing in films grown via pulsed laser deposition, how this intermixing is influenced by the (non)stoichiometry of the growing layers, and the implications for the electronic structure (including the band offsets, band bending, and built-in electric fields).[18,19] Although many researchers have observed these effects, the mechanism for this exotic phenomenon has not been uniquely identified.

Similarly, over the past few years there has been increasing study of $SrTiO_3$ as a candidate thermoelectric material. Much of this work has focused on fine-level control of doped varieties of this material. $SrTiO_3$ is a large band gap semiconductor that can be controllably doped on either the Sr- or the Ti-sites or with O-vacancies to achieve n-type carriers. For thermoelectric applications, one must maximize the figure of merit for thermoelectrics (ZT) which is defined as $(S^2\sigma/\kappa)T$ where $S^2\sigma$ is

Received: October 9, 2011
Revised: December 21, 2011
Published: December 26, 2011

the power factor, κ is the thermal conductivity, and T is the temperature. In $SrTiO_3$, the power factor can be as large as 36 $\mu W\ K^{-2}\ cm^{-1}$ near room temperature, comparable with commercial thermoelectrics.[20] The prevailing opinion is that $SrTiO_3$ may be a promising thermoelectric if the thermal conductivity of this material can be reduced. Recently researchers have tried nanostructuring via superlattice formation[21,22] as a way to reduce the thermal conductivity. Furthermore, recent reports of double-doping $SrTiO_3$ suggest improved performance in part arising from a diminished room temperature thermal conductivity.[4] The work to-date does not, however, provide an in-depth discussion of the mechanism for diminished thermal conductivity despite the importance of these observations for the observed improvements in performance.

A the core of these observations, is a growing concern that as we push the limits for growth and characterization of modern thin film materials, we are increasingly observing exotic phenomena that may not be intrinsic properties of materials. These phenomena, however, may be the result of advanced characterization techniques probing our inability to synthesize materials with the precision we desire. In the current work, we investigate the validity of one of the most fundamental assumptions about pulsed laser deposition: that this technique has an exquisite ability to maintain stoichiometric transfer of components from target to film.[23,24] In particular, we examine the laser fluence[25,26] and angular dependence[27] of stoichiometry and the impact of variations in stoichiometry on the structure,[28] dielectric response,[29−31] and thermal conductivity[32] of $SrTiO_3$ thin films. As the interest in thin films of complex oxide materials has blossomed, researchers have pushed the limits of the available growth techniques as they search for control of these materials at the same level as conventional semiconductor materials. In $SrTiO_3$, this has driven a revisit to homoepitaxy[33] and studies of quantum phenomena in homoepitaxial structures including the observation of exceptionally high (>30,000 $cm^2\ V^{-1}\ s^{-1}$) charge-carrier mobility.[34] These studies have required state-of-the-art deposition methods (including custom molecular beam epitaxy techniques)[35] to elicit fine-level control over chemistry, low-temperature transport studies, and more. The majority of work on $LaAlO_3$/$SrTiO_3$ heterointerfaces and $SrTiO_3$-based thermoelectrics, however, is based on pulsed laser deposition which requires equal attention to detail to obtain high-quality films. The current work develops a better understanding of the effect of variations in the pulsed laser deposition growth parameters (especially laser fluence and growth geometry) on the chemistry and properties of intrinsic $SrTiO_3$ thin films. The current work examines a number of nondestructive characterization routes by which we can examine the chemistry, structural quality, and physical properties of instrinsic-$SrTiO_3$ films.

EXPERIMENTAL SECTION

Thin films of $SrTiO_3$ were grown via pulsed laser deposition using a KrF excimer laser (LPX 205, Coherent) at 750 °C (temperature measured by a thermocouple embedded in the heater block) in 100 mTorr of oxygen pressure from a single crystal $SrTiO_3$ target. Films were grown on $SrTiO_3$ (001), $NdGaO_3$ (110), and 0.5% Nb-doped $SrTiO_3$ (001) single crystal substrates attached to the heater block via Ag paint (Ted Pella, Inc.). A laser spot size of 0.19 cm^2 was used for the growth of all films and by changing the laser energy the laser fluence was varied between 0.35 and 0.69 J/cm^2. Films grown at 0.35 J/cm^2 were grown at 15 Hz and films grown at fluences in excess of 0.35 J/cm^2 were grown at 5 Hz. We note that this variation in laser repetition rate was found to have a negligible effect on the properties reported here. Laser fluence was determined by measuring the laser energy with a calibrated, external energy meter, and the ablation spot size was measured via optical techniques. The target for this study was a 0.5 mm thick $SrTiO_3$ (001) single crystal (Crystec, GmbH). Consistent with previous studies,[25,26] the target was sanded, cleaned, and sufficiently preablated to ensure the target surface had reached steady state prior to growth. The on-axis target-substrate distance was maintained at 6.35 cm for all depositions. Substrates were placed at different locations upon the heater block to vary deposition angle (which resulted in small deviations in target-substrate distance) (Figure 1a). As part of this study we have investigated films between

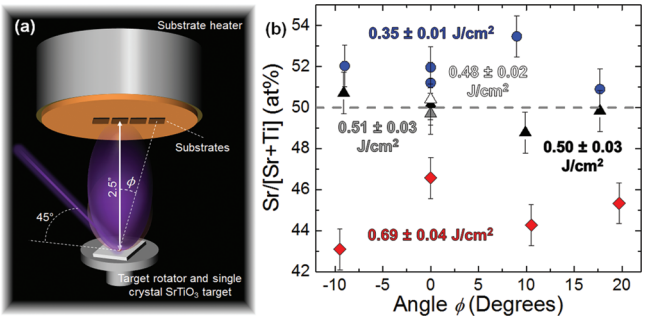

Figure 1. (a) Schematic illustration of deposition geometry. (b) Summary of XPS results for SrTiO3 films grown on $NdGaO_3$ substrates. Graph shows the atomic percentage of Sr (Sr/[Sr+Ti]) as a function of growth geometry and laser fluence. The dashed line indicates XPS results for bulk, stoichiometric $SrTiO_3$.

50 and 320 nm in thickness. Following growth, films were cooled at 5 °C/min to room temperature in 700 Torr of oxygen to promote oxidation.

Films were characterized by an array of techniques to probe their chemical, structural, electrical, and thermal properties. Chemical analysis of samples was completed using a combination of X-ray photoelectron spectroscopy (XPS, Kratos Axis XPS, monochromatic Al X-ray source with charge neutralization during collection via electron beam bombardment) and Rutherford backscattering spectrometry (RBS, incident ion energy of 2000 keV, incident angle α = 22.5°, exit angle β = 52.5°, and a scattering angle θ = 150°). Structural studies were completed using high-resolution X-ray diffraction and reciprocal space mapping (RSM) (Panalytical, X'Pert MRD Pro). Electrical characterization included the study of dielectric constant and loss tangents of 110 nm Pd/200 nm $SrTiO_3$/0.5%Nb-$SrTiO_3$ capacitor structures using an Agilent 4284A LCR meter for frequencies between 10^2−10^5 Hz. Finally, thermal conductivity was probed using time-domain thermoreflectance (TDTR) which is a rapid and accurate way to measure the thermal conductance of interfaces and the thermal conductivity of thin films and bulk materials.[36,37]

RESULTS AND DISCUSSION

We begin by discussing the results of chemical analysis of the cation stoichiometry of these films. One nondestructive technique for characterizing film composition is to measure core-level photoelectron yields via XPS. For this study, we focus on the Sr 3*d* and Ti 2*p* core electron peaks, as those peaks represent the dominant contributions to the XPS signal for $SrTiO_3$ and provide direct insight into the cations of interest (we provide characteristic XPS spectra for a number of samples in Supporting Information, Figure S1). We note that considerable effort was invested to calibrate this system for the study of these and other chemical species including extensive studies of as-received and etched-and-annealed[38,39] versions of the same $SrTiO_3$ single crystals used as targets and

dx.doi.org/10.1021/cm203042q | Chem. Mater. 2012, 24, 331−337

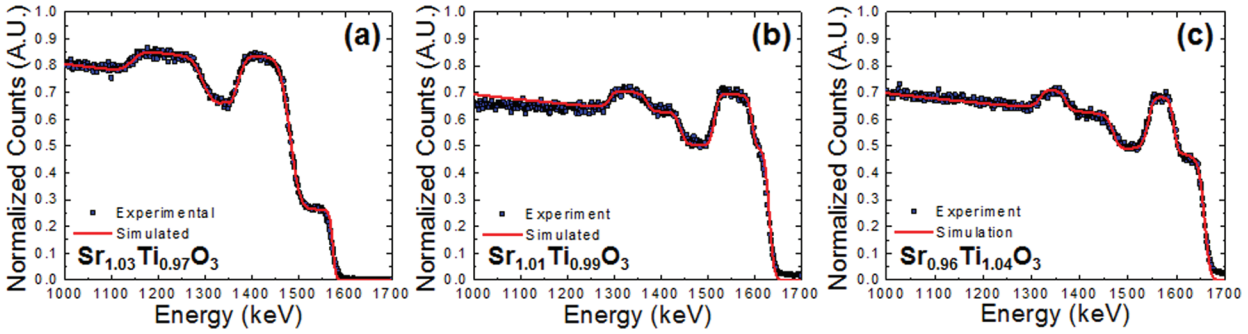

Figure 2. RBS results for $SrTiO_3$ films grown on $NdGaO_3$ (110) substrates at laser fluence (a) 0.35 J/cm^2 [170 nm thick], (b) 0.50 J/cm^2 [70 nm thick], and (c) 0.69 J/cm^2 [50 nm thick] which correspond to Sr atomic-percentages of 52%, 50%, and 48%, respectively.

substrates. Such studies have provided a strong foundation for the current analysis and have been used as a calibration for the 1:1 Sr/Ti cation ratio from XPS (Supporting Information, Figure S1).

The XPS data provide an overview of the results of this study (Figure 1b). The XPS data suggest that in the growth of $SrTiO_3$ films from a $SrTiO_3$ single crystal target that there is not a strong angular dependence in the composition. This is in contrast to previous studies on $LaAlO_3$, which have shown a strong relationship between deposition angle and stoichiometry.[40] The discrepancy in behavior may be explained by the large discrepancy of the atomic masses of cations in $LaAlO_3$ (515%) as compared to those in $SrTiO_3$ (183%). Early studies focusing on growth from ceramic $SrTiO_3$ targets (which show dramatically different laser fluence dependence as compared to single crystal targets)[25−27,29] also exhibit minimal angle dependence. Large deviations in stoichiometry, however, are seen to occur from even relatively small variations in the laser fluence. This strong relationship between fluence and stoichiometry has been observed in previous studies of $SrTiO_3$ homoepitaxy.[25,26] We observe that intermediate laser fluence (i.e., 0.50 J/cm^2) yields films with nearly stoichiometric 1:1 Sr/Ti ratios. The trends observed here are consistent with prior studies which have suggested an optimum laser fluence considerably less than 1 J/cm^2 at which stoichiometric films are obtained. Note that deviations from this value are expected considering differences in the lasers used in the deposition process between papers (e.g., differences in pulse duration, pulse-to-pulse energy stability, beam profile, beam divergence, etc.).[25] Increasing the laser fluence beyond this threshold yields Sr-deficient films (red data, Figure 1b) and decreasing the laser fluence below this threshold yields films with Sr-excess (blue data, Figure 1b).

It is worth noting that ∼95% of the signal in these XPS studies comes from the top few nanometers (<5 nm) of the film. Thus, further studies of stoichiometry throughout the film thickness were done via RBS. We focus on a series of on-axis samples (ϕ = 0°, Figure 1b) to further investigate the effect of laser fluence on the cation stoichiometry and to validate the range of stoichiometries observed here. Consistent with the XPS data, RBS studies of films grown at 0.35 J/cm^2 (Figure 2a), 0.50 J/cm^2 (Figure 2b), and 0.69 J/cm^2 (Figure 2c) are found to exhibit Sr-excess (52 atomic-percent Sr), a nearly 1:1 Sr/Ti ratio (50 atomic-percent Sr), and Sr-deficiency (48 atomic-percent Sr), respectively. The fits of the RBS spectra have an uncertainty of 1.2%, but match the cation stoichiometry from XPS to within 0.5%. Cross-correlated XPS/RBS studies were done on nearly 10 samples with similar results. We provide further analysis and demonstration of RBS sensitivity in the Supporting Information, Figure S2. Thus two different methods, one probing near surface chemistry and one probing through-thickness chemistry, reveal similar trends in the variation of cation stoichiometry in $SrTiO_3$ thin films with variations in fluence and angle of deposition.

The idea that pulsed laser deposition can result in nonstoichiometric films is not new. As early as 1998 initial studies suggested that varying laser fluence in the growth of $SrTiO_3$ from polycrystalline targets could result in non-stoichiometric films.[27] These results suggested that at low laser fluence (<1.3 J/cm^2) preferential ablation of Sr occurred from the ceramic targets, resulting in nonstoichiometric films. Likewise, much of the work on $SrTiO_3$-based thermoelectrics over the years has also focused on doped-$SrTiO_3$ ceramic targets, and the literature provides an incomplete description of growth processes to assess the resulting film chemistry. Over the years, researchers have predominantly switched to single crystal $SrTiO_3$ targets, but with similar results.[25] More recently work on exotic phenomena at the $LaAlO_3/SrTiO_3$ interface has seen researchers focus on specific film growth parameters that give rise to interfacial conductivity, especially growth from single crystal targets at laser fluence well in excess of 0.7 J/cm^2 (some as high as 1.6 J/cm^2).[19] Although it is difficult to accurately compare individual growth systems, a number of reports suggest that growth from single crystal $SrTiO_3$ targets at laser fluence in excess of 0.5−0.6 J/cm^2 results in Sr-deficient thin films. Despite the important implications for materials properties, the trend has been to assume correct stoichiometric transfer and to focus on advanced characterization studies. Here we present a number of techniques that can be used to quickly characterize the stoichiometry of films prior to such in-depth physical property studies.

We used X-ray diffraction to characterize the structure of the films. The out-of-plane lattice parameter of the films was investigated by 2θ scans about the 110/220 and 001/002 diffraction peaks of $NdGaO_3$ and $SrTiO_3$, respectively. Reciprocal space maps about the pseudocubic 103 and 013 diffraction conditions of the film and substrate were taken to determine the in-plane lattice parameters of the film and provide a clear picture of the strain state. Wide range 2θ scans for the same films studied by XPS/RBS revealed the presence of single-phase, 00l-oriented $SrTiO_3$ films in all cases (Supporting Information, Figure S3). No evidence for any Ruddlesden−Popper series phases or TiO_2 was observed suggesting the films, in all cases, are either within the effective solubility limit for Sr-excess and -deficiency or possess fractions of these phases below the sensitivity of the diffraction

dx.doi.org/10.1021/cm203042q | Chem. Mater. 2012, 24, 331−337

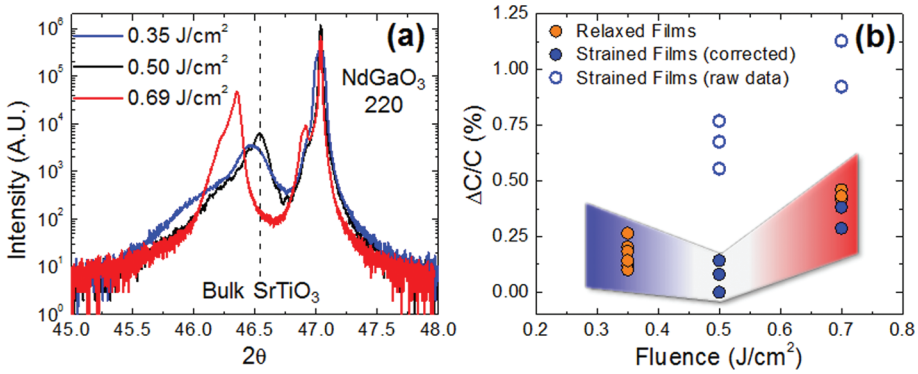

Figure 3. (a) Shows 2θ scans of the 002 diffraction peaks for $SrTiO_3$ films grown at three different laser fluences: 0.35, 0.50, and 0.69 J/cm^2. (b) Change in *c*-axis lattice parameter of a number of $SrTiO_3$ thin films. Films found to be strained have been corrected based on reciprocal space maps and subsequent calculation of strain-free intrinsic lattice parameter. Direct comparison of filled circles suggests a symmetric lattice parameter change with excess Sr or Ti, but an asymmetric strain relaxation mechanism. In general stoichiometric and Ti-rich films are found to remain coherent strained to thicker films.

experiments. Close inspection of the 002-diffraction peak of the $SrTiO_3$ films (Figure 3a) demonstrates that small variations in the laser fluence result in dramatically different structures. Similar results were observed for homoepitaxial $SrTiO_3$ films.[25] Figure 3b shows the intrinsic, stress-free out-of-plane lattice for all films as a function of laser fluence. Films were found to fall into one of two categories: fully relaxed (i.e., taking on the intrinsic in-plane lattice parameters expected for that composition) and strained (i.e., coherently matched to the underlying substrate's in-plane lattice parameters) films. The data here are for films grown on $NdGaO_3$ (110) substrates (which allows us to accurately observe the $SrTiO_3$ diffraction peaks without concern for peak overlap with the substrate). $NdGaO_3$ has slightly anisotropic in-plane lattice parameters a = 3.86 Å and b = 3.85 Å that are somewhat smaller than the lattice parameter of $SrTiO_3$ (a = 3.905 Å). This results in an effective in-plane compressive strain on the $SrTiO_3$ thin films and an expectation of larger out-of-plane lattice parameters for the $SrTiO_3$ films.

Analysis of these data suggest an asymmetric response in terms of structural evolution depending upon the nature of the nonstoichiometry. In particular, films that were (nearly) stoichiometric or Sr-deficient revealed significantly enlarged out-of-plane lattice parameters (0.5 and 0.69 J/cm^2, open circles in Figure 3b), while those films known to possess a Sr-excess consistently showed nearly intrinsic out-of-plane lattice parameters (0.35 J/cm^2, Figure 3b). All films were then analyzed using RSM to probe the in-plane strain state of the film (typical RSM data for a variety of laser fluences and film thicknesses are provided in Supporting Information, Figure S4). In general, it was found that films possessing a Sr-excess quickly relaxed to the bulk-like in-plane lattice parameters at thicknesses >50 nm. On the other hand, stoichiometric and Sr-deficient samples were found to remain strained up to thicknesses of ~200 nm. For films found to be strained to the substrate by RSM analysis, we have calculated the intrinsic, stress-free lattice parameter (a_0) using

$$a_0 = \frac{(1-\nu)a_z + \nu(a_x + a_y)}{1+\nu} \quad (1)$$

where ν is the Poisson's ratio of $SrTiO_3$, here assumed to be 0.2,[41] a_z is the strained out-of-plane lattice parameter of the film, and a_x and a_y are the in-plane lattice constants of the pseudocubic $NdGaO_3$ lattice. Using this equation we have corrected the strained film lattice parameters (open circles, Figure 3b) to allow direct comparison with the fully relaxed films (blue filled circles, Figure 3b).

This data suggests an important limitation to X-ray diffraction based studies of nonstoichiometric films. Specifically X-ray diffraction alone can only tell you that your film is off-stoichiometric, but does not provide insight into the nature of that off-stoichiometry. The general trend of increasing lattice parameter with increasing off-stoichiometry has been observed previously and is thought to be the result of the formation of disordered planar-like SrO faults in the case of low-fluence (Sr-excess) and Sr-vacancies in the case of high-fluence (Sr-deficient) films.[28] Furthermore, recent studies have observed that in films grown on $SrTiO_3$ (001) substrates with a sufficient density of Ti-vacanices (Sr-excess), expansion and elongation of the lattice parameters may also occur.[42] The tendency for Sr-excess films to relax at considerably thinner film thicknesses than stoichiometric or Sr-deficient films could result for a number of reasons. Sr-excess may change the energy barrier of formation of dislocations, formation of planar-like SrO faults could help nucleate strain-relaxing dislocations, or strain could be accommodated by the disordered planar-like SrO faults that run perpendicular to the surface of the substrate themselves. Analysis of highly off-stoichiometric films suggests the possibility of forming 3D networks of these structures is unlikely since local lattice distortions might drive the structure energetically unstable and models suggested layered planar-like SrO faults might be more favorable.[28] More recent work on molecular beam epitaxy grown films suggests alignment of these layered planar-like SrO features perpendicular to the substrate surface[33] which might represent an alternative mode of strain relaxation. The absence of similar layered structures in Sr-deficient films might preclude this mechanism of strain relaxation and allow thicker films to remain coherently strained.

We have gone on to probe the effect of this non-stoichiometry on the dielectric and thermal properties of these films. We begin here with a discussion of the effect of stoichiometry on dielectric response. Over the years, the dielectric properties of $SrTiO_3$ thin films have traditionally been found to be diminished when compared to bulk samples of $SrTiO_3$. Early studies of permittivity in $SrTiO_3$ thin films as a function of composition suggested a possible explanation.[29−31] These early reports focused on growth from compositionally

dx.doi.org/10.1021/cm203042q | *Chem. Mater.* 2012, 24, 331−337

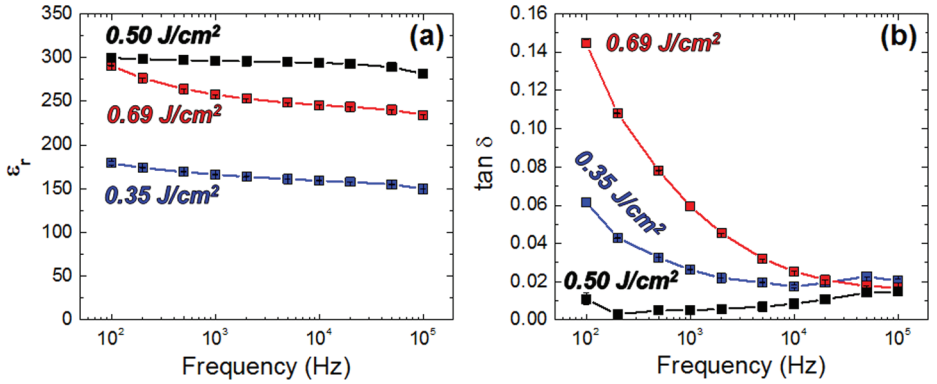

Figure 4. (a) Low-frequency dielectric constant for Pd/$SrTiO_3$/Nb:$SrTiO_3$ (001) films grown at 0.35, 0.50, and 0.69 J/cm^2. (b) Corresponding loss tangent as a function of frequency. Error bars are present in both figures, but are too small to see on this scale.

varied ceramic targets and suggested somewhat contradictory results for optimal properties. For instance, one study suggested that 10% excess Ti was needed in the target to obtain bulk-like ε_r at 300 K[21] while others observed a dramatic increase in dielectric response with targets possessing either Sr- or Ti-excess,[29] and still others suggested the need for laser fluence as large as 5 J/cm^2 to achieve bulk-like dielectric response.[30] In no case has a report provided measures of film stoichiometry (as opposed to target stoichiometry) and the connection to dielectric response; and none of these reports provide significant details concerning the effect of nonstoichiometry, the resulting defect types, and properties.

Low-frequency ε_r and tan δ (10^2–10^5 Hz) were estimated from capacitance–voltage measurements across this frequency range. The room temperature ε_r of stoichiometric films grown at 0.50 J/cm^2 was found to be ~300 and was essentially constant across the 4 decades of frequency studied here (black data symbols, Figure 4a). Moving to higher laser fluence (Sr-deficient films) resulted in a slight decrease in the overall magnitude of ε_r and a more noticeable frequency dependence across the range studied (red data symbols, Figure 4a). Likewise, transitioning to lower laser fluence (Sr-excess films) resulted in the most significant decrease in permittivity (blue data symbols, Figure 4a). Consistent effects were observed in the losses (tan δ), with the most pronounced differences occurring at low frequencies (Figure 4b). We note that although all off-stoichiometry films were found to have high loss levels, the relative increase in loss was not directly correlated to the loss in permittivity. In fact, films with Sr-deficiency are found to have the largest losses in all cases. Similar dramatic effects on electrical properties have been observed in Nb-doped $SrTiO_3$ thin films where growth-induced nonstoichiometry resulted in order of magnitude increases in the electrical resistance.[26]

Overall there are likely a number of competing factors that give rise to these changes in dielectric response. First, generation of increased defect concentrations and lower crystalline quality samples (which coincide with off-stoichiometry) are known to reduce dielectric response and lead to increases in losses. Second, the formation of other phases (i.e., the disordered planar-like SrO faults) which have lower static dielectric constants effectively lowers the overall response of the system. The static dielectric constant of SrO is 13.1 (at 10 kHz).[43] Using a simple model of series capacitors for the composite film and using the known Sr-excess to estimate the fraction of volume occupied by the planar-like SrO-phase, we can estimate the reduction in the permittivity. Within the error of the stoichiometry measurements (±1.2%) we calculate an estimated permittivity for the $SrTiO_3$/planar-like SrO faults composite films to be 150±15. This matches well with the experimentally observed values. The slight discrepancy could be explained by the fact that not all of the excess Sr may be present in the planar-like SrO faults, but some could be accommodated (along with Ti-vacancies) in the $SrTiO_3$ or that some fraction of the planar-like SrO faults are running parallel to the measurement direction and do not contribute equally to the loss of dielectric response. Sr-deficient films on the other hand are thought to accommodate more Sr-vacancies and do not form a Ti-rich second phase until larger off-stoichiometry. This results in a diminished permittivity, but not to the same extent as Sr-excess films. The difference in these defect structures, also gives rise to a large difference in tan δ. The Sr-deficient samples (which are thought to possess an increased concentration of Sr- and O-vacancies) show a slight decrease in ε_r, but a dramatic increase in tan δ, consistent with the production of excess charge carriers and significantly increased losses. On the other hand, Sr-excess samples (which are thought to possess disordered planar-like SrO faults) experience a dramatic reduction of ε_r, but only limited enhancement of losses consistent with only a nominal increase in charge carrier concentration in the film.

Thermal conductivity was measured via TDTR. A coating of ~100 nm of Al was used as the optical transducer for all measured samples. The results for these characterizations are summarized in Figure 5. The thermal conductivity of the films shows a strong correlation to laser fluence, and therefore, film composition. Nearly stoichiometric films grown at a laser fluence of 0.50 J/cm^2 show the highest as-grown thermal conductivity. Increasing the laser fluence by 28% to 0.69 J/cm^2 (resulting in a ~2–4% Sr-deficiency) results in a reduction of the thermal conductivity by ~35% compared to stoichiometric films. Likewise, reduction of the laser fluence by 30% to 0.35 J/cm^2 (resulting in a ~2–4% Sr-excess) reduces the thermal conductivity in the film by nearly 65% as compared to the stoichiometric films. Much like the epitaxial strain relaxation process, the deviation in thermal conductivity is found to be highly asymmetric, with small deviations toward Sr-excess driving dramatic changes in thermal conductivity. The thermal conductivity of $SrTiO_3$ is dominated by the phonon contribution,[44] and the observed effect of stoichiometry on this thermal conductivity is a direct manifestation of the impact of how defects in materials impact phonons. Recall that films

dx.doi.org/10.1021/cm203042q | Chem. Mater. 2012, 24, 331–337

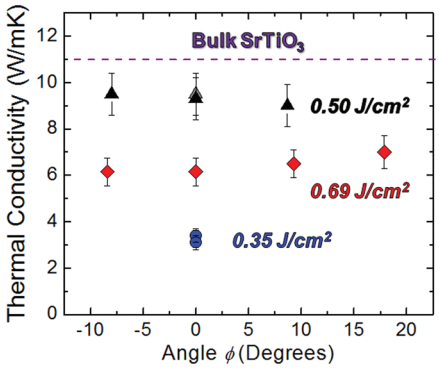

Figure 5. TDTR results for $SrTiO_3$ films grown on $NdGaO_3$ (110) substrates as a function of deposition geometry and laser fluence. The dashed line indicates the thermal conductivity of bulk $SrTiO_3$. In general, films with excess Sr (blue circles) exhibit a drastic reduction of thermal conductivity, those with excess Ti (red diamonds) show a somewhat diminished thermal conductivity, and nearly stoichiometric (black triangles) show the highest thermal conductivity.

possessing Sr-deficiency have an enhanced concentration of Sr vacancy point defects. Such point defects tend to scatter higher frequency phonons, leading to a smaller, but non-negligible reduction in thermal conductivity. On the other hand, however, Sr-excess results in the formation of disordered planar-like SrO faults which lead to an increase in crystalline interfaces throughout the film.[28,33] These interfaces cause increased scattering rates of all phonons, producing a much larger reduction of thermal conductivity.

We also note that the nearly stoichiometric films show thermal conductivities somewhat diminished from the bulk thermal conductivity of $SrTiO_3$.[32] A number of important considerations should be discussed. First, the data here is for films grown on $NdGaO_3$ (110) substrates and represent a range of strained and unstrained films. It is thought that the extended defects and residual strain created by growth on a lattice mismatched substrate should not have a significant effect on thermal conductivity at temperatures $T > 150$ K. This weak strain effect can be explained by the Leibfried−Schlomann equation which states that the thermal conductivity should scale with the cube of the Debye temperature.[45,46] The Grüneisen parameter of $SrTiO_3$ is 1.5[47] and thus a strain of 1.1% (consistent with a coherently strained film on $NdGaO_3$) should produce only a 1.7% change in the Debye temperature, and therefore a 5.1% increase in thermal conductivity. This cannot explain the nearly 14% reduction in thermal conductivity observed for the stoichiometric films. Furthermore, because some films are fully strained, some partially relaxed, and others completely relaxed, a more dramatic variation in results would be expected if strain was producing a dramatic effect. We believe that the diminished thermal conductivity can be explained by the effects of oxygen vacancies. Upon annealing the nearly stoichiometric samples in 760 Torr of O_2 at 700 °C for 2 h, we observe the thermal conductivity to be enhanced relative to the as-grown samples. Similar changes in thermal conductivity were observed in significantly oxygen deficient single crystal $SrTiO_3$.[48]

CONCLUSION

We have shown that the stoichiometry of $SrTiO_3$ thin films grown via pulsed laser deposition can vary dramatically from the expected. In particular, the laser fluence has a marked effect on the stoichiometry and small variations in laser fluence can drastically change the stoichiometry. Furthermore, these compositional variations can lead to diminished structural quality and, in turn, diminished dielectric and thermal properties.

Recent work on $LaAlO_3/SrTiO_3$ heterointerfaces and $SrTiO_3$-based thermoelectrics has provided exciting possibilities for new devices and applications based on oxide materials. In the pursuit of these exciting results, however, researchers may have overestimated the robustness of our synthesis methods. In an effort to fully understand the mechanisms behind these intriguing phenomena, we cannot overlook basic materials concepts such as (non)stoichiometry and the importance of these effects in determining our ultimate performance. Regardless of the fundamental mechanism for such effects, researchers are finding innovative ways to utilize such phenomena in first generation devices. Nonetheless, by combining two or more of the techniques of X-ray diffraction, dielectric response, and thermal characterization researchers can accurately probe cation stoichiometry in these intrinsic (i.e., undoped) complex oxide systems. In the end, it is important for researchers to fully understand how failures in our assumptions about deposition techniques can impact the properties of the samples produced. How such stoichiometric deviations could result in the manifestation of a range of exotic phenomena observed in $SrTiO_3$-based systems is beyond the scope of this paper, but what is clear is that such deviations must be carefully studied in these exciting systems to uniquely identify the fundamental mechanisms for these important phenomena.

ASSOCIATED CONTENT

Supporting Information

Full information about XPS spectra, RBS fit sensitivity, wide-angle XRD scans, and reciprocal space maps of relevant films. This material is available free of charge via the Internet at http://pubs.acs.org.

AUTHOR INFORMATION

Corresponding Author

*Phone: 217-244-9162. E-mail: lwmartin@illinois.edu.

ACKNOWLEDGMENTS

The authors would like to acknowledge the help and scientific insights of Rick Haasch and Doug Jeffers at the Center for Microanalysis of Materials at UIUC. The work was supported by the U.S. Department of Energy under Grant DEFG02-07ER46459. Experiments at UIUC were carried out in part in the Frederick Seitz Materials Research Laboratory Central Facilities, which are partially supported by the U.S. Department of Energy under Grants DE-FG02-07ER46453 and DE-FG02-07ER46471.

REFERENCES

(1) Muller, K. A.; Burkard, H. *Phys. Rev. B* **1979**, *19*, 3593.
(2) Frederikse, H. P. R; Thurber, W. R.; Hosler, W. R. *Phys. Rev.* **1964**, *134*, A442.
(3) Jalan, B.; Stemmer, S. *Appl. Phys. Lett.* **2010**, *97*, 042106.
(4) Ravichandran, J.; Siemons, W.; Oh, D.-W.; Kardel, J. T.; Chari, A.; Heijmerikx, H.; Scullin, M. L.; Majumdar, A.; Ramesh, R.; Cahill, D. G. *Phys. Rev. B* **2010**, *82*, 165216.
(5) Tufte, O. N.; Chapman, P. W. *Phys. Rev. B* **1967**, *155*, 796.
(6) Frederikse, H. P. R; Hosler, W. R. *Phys. Rev.* **1967**, *161*, 822.

(7) Takahashi, K. S.; Gabay, M.; Jaccard, D.; Shibuya, K.; Ohnishi, T.; Lippmaa, M.; Triscone, J.-M. *Nature* **2006**, *441*, 195.
(8) Shibuya, K.; Ohnishi, T.; Uozumi, T.; Sato, T.; Lippmaa, M.; Kawasaki, M.; Nakajima, K.; Chikyow, T.; Koinuma, H. *Appl. Phys. Lett.* **2006**, *88*, 212116.
(9) Ohtomo, A.; Hwang, H. Y. *Nature* **2004**, *427*, 423.
(10) Brinkman, A.; Huijben, M.; van Zalk, M.; Huijben, J.; Zeitler, U.; Maan, J. C.; van der Wiel, W. G.; Rijnders, G.; Blank, D. H. A.; Hilgenkamp, H. *Nat. Mater.* **2007**, *6*, 493.
(11) Reyren, N.; Thiel, S.; Caviglia, A. D.; Fitting-Kourkoutis, L.; Hammerl, G.; Richter, C.; Schneider, C. W.; Kopp, T.; Rüetschi, A.-S.; Jaccard, D.; Gabay, M.; Muller, D. A.; Triscone, J. M.; Mannhart, J. *Science* **2007**, *317*, 1196.
(12) Singh-Bhalla, G.; Bell, C.; Ravichandran, J.; Siemons, W.; Hikita, Y.; Salahuddin, S.; Hebard, A. F.; Hwang, H. Y.; Ramesh, R. *Nat. Phys.* **2011**, *7*, 80.
(13) Park, J. W.; Bogorin, D. F.; Cen, C.; Felker, D. A.; Zhang, Y.; Nelson, C. T.; Bark, C. W.; Folkman, C. M.; Pan, X. Q.; Rzchowski, M. S.; Levy, J.; Eom, C. B. *Nat. Commun.* **2010**, *1*, 94.
(14) Cen, C.; Thiel, S.; Hammerl, G.; Schneider, C. W.; Andersen, K. E.; Hellberg, C. S.; Mannhart, J.; Levy, J. *Nat. Mater.* **2008**, *7*, 298.
(15) Breitschaft, M.; Tinkl, V.; Pavlenko, N.; Paetel, S.; Richter, C.; Kirtley, J. R.; Liao, Y. C.; Hammerl, G.; Eyert, V.; Kopp, T.; Mannhart, J. *Phys. Rev. B* **2010**, *81*, 153414.
(16) Herranz, G.; Basleti, M.; Bibes, M.; Carrétéro, C.; Tafra, E.; Jacquet, , E.; Bouzehouane, , K.; Deranlot, , C.; Hamzi, A.; Broto, J.-M.; Barthélémy, A.; Fert, A. *Phys. Rev. Lett.* **2007**, *98*, 216803.
(17) Willmott, P. R.; Pauli, S. A.; Schlepütz, C. M.; Martoccia, D.; Patterson, B. D.; Delley, B.; Clarke, R.; Kumah, D.; Cionca, C.; Yacoby, Y. *Phys. Rev. Lett.* **2007**, *99*, 155502.
(18) Qiao, L.; Droubay, T. C.; Kaspar, T. C.; Sushko, P. V.; Chambers, S. A. *Surf. Sci.* **2011**, *605*, 1381.
(19) Chambers, S. A.; Englhard, M. H.; Shutthanandan, V.; Zhu, Z.; Droubay, T. C.; Qiao, L.; Sushko, P. V.; Feng, T.; Lee, T. D.; Gustafsson, T.; Garfunkel, E.; Shah, A. B.; Zuo, J.-M.; Ramasse, Q. M. *Surf. Sci. Rep.* **2010**, *65*, 317.
(20) Okuda, T.; Nakanishi, K.; Miyasaka, S.; Tokura, Y. *Phys. Rev. B* **2001**, *63*, 113104.
(21) Ohta, H.; Kim, S.; Mune, Y.; Mizoguchi, T.; Nomura, K.; Ohta, S.; Nomura, T.; Nakanishi, Y.; Ikuhara, Y.; Hirano, M.; Hosono, H.; Koumoto, K. *Nat. Mater.* **2007**, *6*, 129.
(22) Mune, Y.; Ohta, H.; Koumoto, K.; Mizoguchi, T.; Ikuhara, Y. *Appl. Phys. Lett.* **2007**, *91*, 192105.
(23) Dijkkamp, D.; Venkatesan, T.; Wu, X. D.; Shaheen, S. A.; Jisrawi, N.; Min-Lee, Y. H.; McLean, W. L.; Croft, M. *Appl. Phys. Lett.* **1987**, *51*, 619.
(24) Lowndes, D. H.; Geohegan, D. B.; Puretzky, A. A.; Norton, D. P.; Rouleau, C. M. *Science* **1996**, *273*, 898.
(25) Ohnishi, T.; Lippmaa, M.; Yamamoto, T.; Meguro, S.; Koinuma, H. *Appl. Phys. Lett.* **2005**, *87*, 241919.
(26) Ohnishi, T.; Shibuya, K.; Yamamoto, T.; Lippmaa, M. *J. Appl. Phys.* **2008**, *103*, 103703.
(27) Dam, B.; Rector, J. H.; Johansson, J.; Huijbregtse.; De Groot, D. B. *J. Appl. Phys.* **1998**, *83*, 3386.
(28) Suzuki, T.; Nishi, Y.; Fujimoto, M. *Philos. Mag. A* **2000**, *80*, 621.
(29) Hirano, T.; Taga, M.; Kobayashi, T. *Jpn. J. Appl. Phys.* **1993**, *32*, L1760.
(30) Ota, H.; Migita, H.; Xiong, S.-B.; Kasai, Y.; Sakai, S. *Jpn. J. Appl. Phys.* **1999**, *38*, L1535.
(31) Lippmaa, M.; Nakagawa, N.; Kawasaki, M.; Ohashi, S.; Koinuma, H. *J. Electroceram.* **2000**, *4*, 365.
(32) Oh., D.-W.; Ravichandran, J.; Liang., C.-W.; Siemons, W.; Jalan, B.; Brooks, C. M.; Huijben, M.; Schlom, D. G.; Stemmer, S.; Martin, L. W.; Majumdar, A.; Ramesh, R.; Cahill, D. G. *Appl. Phys. Lett.* **2011**, *98*, 221904.
(33) Brooks, C. M.; Fitting Kourkoutis, L.; Heeg, T.; Schubert, J.; Muller, D. A.; Schlom, D. G. *Appl. Phys. Lett.* **2009**, *94*, 162905.
(34) Son, J.; Moetakef, P.; Jalan, B.; Bierwagen, O.; Wright, N. J.; Engel-Herbert, R.; Stemmer, S. *Nat. Mater.* **2010**, *9*, 482.
(35) Jalan, B.; Engel-Herbert, R.; Wright, N. J.; Stemmer, S. *J. Vac. Sci. Technol. A* **2009**, *27*, 461.
(36) Cahill, D. G.; Ford, W. K.; Goodson, K. E.; Mahan, D. G.; Majumdar, A.; Maris, H. J.; Merlin, R.; Phillpot, S. R. *J. Appl. Phys.* **2003**, *93*, 793.
(37) Cahill, D. G. *Rev. Sci. Instrum.* **2004**, *75*, 5119.
(38) Kawasaki, M.; Takahashi, K.; Maeda, T.; Tsuchiya, R.; Shinohara, M.; Ishiyama, O.; Yonezawa, T.; Yoshimoto, M.; Koinuma, H. *Science* **1994**, *266*, 1540.
(39) Ohnishi, T.; Shibuya, K.; Lippmaa, M.; Kobayashi, D.; Kumigashira, H.; Oshima, M.; Koinuma, H. *Appl. Phys. Lett.* **2004**, *85*, 272.
(40) Droubay, T. C.; Qiao, L.; Kaspar, T. C.; Engelhard, M. H.; Shutthanandan, V.; Chambers, S. A. *Appl. Phys. Lett.* **2010**, *97*, 124105.
(41) Hachemi, A.; Hachemi, H.; Ferhat-Hamida, A.; Louail, L. *Phys. Scr.* **2010**, *82*, 025602.
(42) Keeble, D. J.; Wicklein, S.; Dittmann, R.; Ravelli, L.; Mackie, R. A.; Egger, W. *Phys. Rev. Lett.* **2010**, *105*, 226102.
(43) Jacobson, J. L.; Nixon, E. R. *J. Phys. Chem. Sol.* **1968**, *29*, 967.
(44) Cahill, D. G.; Pohl, R. O. *Annu. Rev. Phys. Chem.* **1988**, *39*, 93.
(45) Roufosse, M.; Klemens, P. G. *Phys. Rev. B* **1973**, *7*, 5379.
(46) Slack, G. A. *Solid State Physics*; Academic Press: New York, 1979.
(47) Beattie, A. G.; Samara, G. A. *J. Appl. Phys.* **1971**, *42*, 2376.
(48) Muta, H.; Kurosaki, K.; Yamanaka, S. *J. Alloys Compd.* **2005**, *392*, 306.